Langmuir

Article

pubs.acs.org/Langmuir

Continuous Droplet Removal upon Dropwise Condensation of Humid Air on a Hydrophobic Micropatterned Surface

Konstantin O. Zamuruyev,[†] Hamzeh K. Bardaweel,[†] Christopher J. Carron,[‡] Nicholas J. Kenyon,[§] Oliver Brand,[‡] Jean-Pierre Delplanque,[†] and Cristina E. Davis*[,†]

[†]Department of Mechanical and Aerospace Engineering, University of California, Davis, Davis, California 95616, United States
[‡]School of Electrical and Computer Engineering, Georgia Institute of Technology, Atlanta, Georgia 30332, United States
[§]Department of Internal Medicine, UC Davis School of Medicine, Davis, California 95616, United States

Supporting Information

ABSTRACT: Combination of two physical phenomena, capillary pressure gradient and wettability gradient, allows a simple two-step fabrication process that yields a reliable hydrophobic self-cleaning condenser surface. The surface is fabricated with specific microscopic topography and further treatment with a chemically inert low-surface-energy material. This process does not require growth of nanofeatures (nanotubes) or hydrophilic−hydrophobic patterning of the surface. Trapezoidal geometry of the microfeatures facilitates droplet transfer from the Wenzel to the Cassie state and reduces droplet critical diameter. The geometry of the micropatterns enhances local coalescence and directional movement for droplets with diameter much smaller than the radial length of the micropatterns. The hydrophobic self-cleaning micropatterned condenser surface prevents liquid film formation and promotes continuous dropwise condensation cycle. Upon dropwise condensation, droplets follow a designed wettability gradient created with micropatterns from the most hydrophobic to the least hydrophobic end of the surface. The surface has higher condensation efficiency, due to its directional self-cleaning property, than a plain hydrophobic surface. We explain the self-actuated droplet collection mechanism on the condenser surface and demonstrate experimentally the creation of an effective wettability gradient over a 6 mm radial distance. In spite of its fabrication simplicity, the fabricated surface demonstrates self-cleaning property, enhanced condensation performance, and reliability over time. Our work enables creation of a hydrophobic condenser surface with the directional self-cleaning property that can be used for collection of biological (chemical, environmental) aerosol samples or for condensation enhancement.

INTRODUCTION

Wettability of a solid surface is one of the most important properties for microfluidic systems. Application of controlled surface wettability for delivery of small amounts of fluid to the desired route in micromixers, pumps, and lab on a chip systems has unlimited potential. It may be the only desired mechanism for certain applications when the input of electrical power is unavailable or can change the properties of the analyte fluid. Wenzel[1] and Cassie[2] proposed and explained wetting regimes of the surfaces with controlled roughness. Patankar et al. developed models and explained the mechanisms for controlled surface wettability with surface roughness, design of self-cleaning surfaces, and droplet transport on micropatterned surfaces with force and energy balance.[3,4] Using these mechanisms, Zhu et al.[5] tuned wettability of the surface by controlling its roughness with well-designed microstructures. Similarly, Yang et al.[6,7] explained droplet manipulation on hydrophobic surface with roughened patterns with conversion of Gibbs energy into kinetic energy. Wier,[8] Dorrer,[9] and Narhe[10] explained the mechanism for droplets nucleation and transition from Wenzel (lower energetic state) to Cassie wetting mode (higher energetic state) in condensation on surfaces roughened with microtopography. Rykaczewski[11,12] explained the three-dimensional aspects of droplet coalescence during dropwise condensation on superhydrophobic surfaces and its contribution to the heat transfer process. Although these topics are understood individually, the combination of two phenomena (wettability gradient for fluid delivery and fluid phase change through condensation) on one surface still represents significant challenges. The small and randomly distributed size of condensate droplets requires a special mechanism for wettability gradient distribution over the sufficiently large area of the condenser surface. The nucleation and growth of droplets on the micropatterned surface decrease their mobility; an effective mechanism is required to transfer them from the immobile "pinned" to the moving state. Few

Received: February 2, 2014
Revised: July 22, 2014
Published: July 29, 2014

   dx.doi.org/10.1021/la5004462 | *Langmuir* 2014, 30, 10133−10142

works have considered the combination of these phenomena for enhancement of continuous condensation cycle on a hydrophobic surface.[13−17] However, it is the combination of these phenomena into a single model that has the potential implications for passively enhanced heat transfer in heat exchangers.[17−21] Also, the self-cleaning condenser surface is useful for collection of biological (chemical, environmental) aerosol samples. First, the conversion to a liquid (denser) phase can facilitate sample manipulation and its chemical analysis when the concentrations are extremely low. Second, this surface can deliver the sample from the collection unit into an interfaced analytical or storage unit with no external power input required. We consider this surface for application in a portable breath analyzer. The surface is installed in the flow chamber and cooled with thermoelectric element under it. The vapor in the exhaled breath is condensed on it as exhaled breath gas passes over it. The exhaled breath condensate droplets are self-delivered into the interfaced analysis sensor.

In this work, we present the design of a self-cleaning hydrophobic condenser surface and a simple two-step technique to fabricate it. Our design approach combines two physical phenomena: a capillary pressure gradient and a wettability gradient. The key feature of this design is the shape, size, and distribution of the microfeatures and trapezoidally shaped grooves and ridges. This geometry and its distribution enhance droplets transfer from the Wenzel to the Cassie state and directional transport over long distances (6 mm). The trapezoidal geometry of the micropatterned grooves and ridges creates a capillary pressure gradient which enables droplet transfer, right after nucleation, from the "pinned" state, inside the groove, to the upper surface of the ridge.[22] This geometry also enhances the wettability gradient distribution on the surface; not only between radial regions but also along the radial length (1 mm) of each region. Upon dropwise condensation, droplets with various sizes, smaller than the micropatterns dimension, follow a designed wettability gradient created with micropatterns from the most hydrophobic to the least hydrophobic end of the surface. The distribution of the wettability gradient was estimated with the contact angle values predicted with the Wenzel and Cassie models based on the designed micropatterns dimensions. Upon fabrication, the force balance was evaluated based on the measured contact angle values and dimensions of the fabricated micropatterns.

This hydrophobic micropatterned condenser surface promotes continuous dropwise condensation cycle and has higher condensation efficiency, due to its directional self-cleaning property, than a plain hydrophobic surface. Removal of condensate droplets from the surface contributes to the heat transfer process by allowing nucleation of multiple droplets on the same site. Droplet removal prevents liquid film formation over the surface.[21] Dropwise condensation is usually preferred to a filmwise condensation regime due to its higher rate of heat transfer.[23,24] A liquid film significantly reduces heat transfer across the surface and lowers condensation efficiency. In dropwise regime, heat transfer between the surface and the humid air is only affected where droplets are present.[25,26] Large patch-like droplets on the surface are undesirable, too, because they hinder the condensation process. Therefore, continuous droplet removal from the condenser surface, before they form a liquid film, maintains dropwise condensation regime with low thermal resistance across the surface and increases condensation efficiency. Maintaining dropwise condensation regime is challenging because droplets tend to coalesce into a liquid film.[17,27] See Video S1 in the Supporting Information for more details on maintaining continuous dropwise condensation cycle.

METHODS

The outer diameter of the condenser surface is 20 mm and consists of six concentric micropatterned circular regions with an 8 mm wide collection point in the center. Both the chemical composition and physical roughness of the condenser surface contribute to its performance. The wettability gradient is obtained by gradually varying the roughness of the surface with micropatterns created by contact photolithography and deep reactive ion etching.[28] The whole condenser surface is then made hydrophobic with a plasma fluorinated polybutadiene film, proposed by Woodward.[27,29] Figure 1 shares more details on the surface fabrication. The fabrication steps and experimental setup are described as follows.

Fabrication of the condenser surface starts with a double-side polished ⟨100⟩ silicon wafer that is baked at 110 °C for 12.5 min to evaporate any moisture. The wafer is spin-coated with a layer of HMDS primer and then with MEGAPOSIT SPR 220-7 photoresist, 12 μm thick. The wafer is soft-baked at 105 °C for 6 min. The micropattern geometries are transferred to the photoresist with contact photolithography. After a 3 h delay to degas any nitrogen trapped in the photoresist, the wafer is softly agitated in CD-26 developer for 5−8 min. The micropatterns are etched into silicon substrate with deep reactive ion etching (model: Alcatel 601E). The wafer is cleaned with acetone, dried with nitrogen, and cleaned further using oxygen plasma for 5 min at 200 W.

The micropatterned surface is coated with a plasma fluorinated polybutadiene film[27,29] to make the surface hydrophobic. Polybutadiene (Aldrich, MW = 420 000, 36% cis 1,4 addition, 55% trans 1,4 addition, 9% 1,2 addition) is dissolved in Toluene (BDH, +99.5% purity) at concentration of 5% (w/w).[27,29] The wafer is spin-coated with the prepared solution at 2000 rpm for 60 s. The thin film is annealed in a vacuum oven for 1 h at 90 °C to remove entrapped solvent. Next, the surface is plasma treated in vacuum chamber for 10 min. Prior to the plasma treatment the chamber is scrubbed with isopropanol followed by further cleaning using oxygen plasma at 200 W for 15 min. Once the chamber reaches its base pressure of 25 mTorr, CF_4 gas is allowed into the chamber and the electrical discharge ignited. The plasma fluorination is carried out at 150 mTorr, 60 W, and 3.0 sccm CF_4 flow rate. To cure the plasma fluorinated polybutadiene film, the wafer is postbaked in a vacuum oven for 1 h at 90 °C. Figure 2 shows the "top view"of the four outermost circular regions of the condenser surface. Specific geometry and distribution of the micropatterns (grooves and ridges) create a wettability gradient toward the center of the condenser surface. Roughness of the surface is controlled with the width of the grooves while the geometry of the ridges is kept the same in all six regions. The interlocking interface of regions is crucial for effective droplet movement.

Upon fabrication, the self-cleaning property of the surface was verified with droplet self-actuated movement on dry surface and in condensation. We want to emphasize an important difference between a self-cleaning surface and a self-cleaning condenser surface because some surfaces lose their ability to actuate droplet movement once they are wetted in condensation. Actuation of droplet motion on a dry surface is one of the initial requirements for a self-cleaning condenser surface. The surface is defined dry if it is not cooled and no condensation occurs on it. The self-cleaning property of the dry surface is characterized by measuring contact angle (CA) at each micropatterned region of the surface. A droplet of deionized water with a volume of 1−2 μL is deposited on each micropatterned circular region, and its contact angle is measured with a goniometer (Ramé-hart Model 250). Droplet profiles and measured static contact angles are shown in Figure 4a.

Droplet mobility on the dry surface is measured by placing a droplet of deionized water with a volume of 3 μL at the outer, most hydrophobic, region of the surface and letting it flow along the wettability gradient, toward the collection point. The droplet movement is captured with a video camera, 29 frames/s, coupled

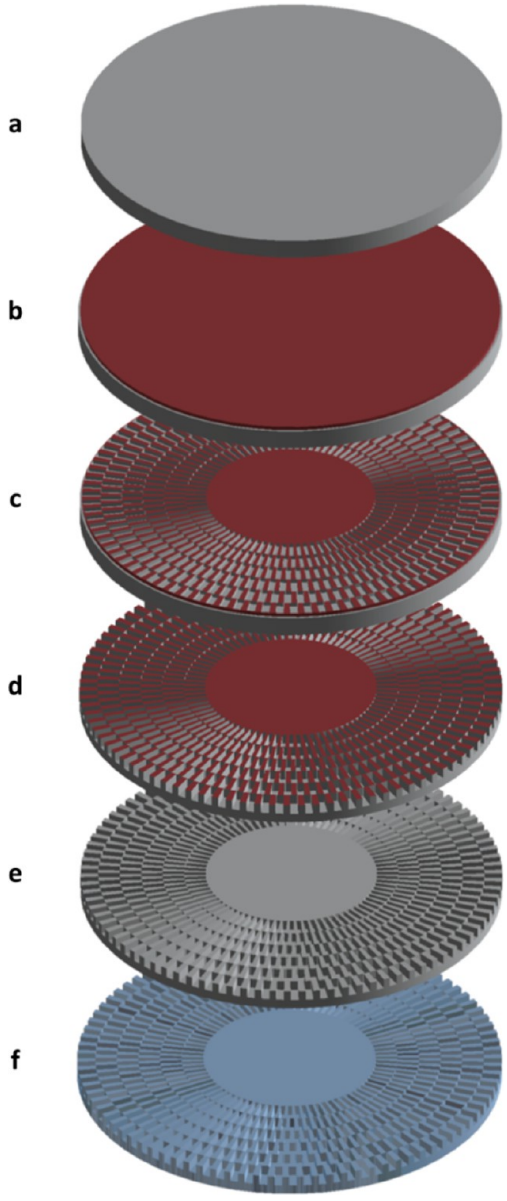

Figure 1. Microfabrication process flow of MEMS based self-cleaning condenser surface. (a) Double-side polished silicon wafer. (b) Spin-coat the wafer with HDMS primer and photoresist. (c) Define the micropatterns with contact photolithography and photoresist development. (d) Etch micropatterns with deep reactive ion etching (DRIE). (e) The wafer is cleaned with acetone, dried with nitrogen, and cleaned further using oxygen plasma for 5 min at 200 W. (f) Spin-coat the wafer with polybutadiene, followed by vacuum annealing, plasma treatment, and postbaking.

with the goniometer. Droplet movement, velocity, and dynamic contact angle (Figure 6) are obtained from the images (frames) extracted from the video files. The droplet displacement is evaluated from the distance between a set point and the droplet as time progresses from frame to frame. Velocity is evaluated as the rate of displacement with respect to time. Image frames are extracted from the video files with Matlab. Droplet displacement and dynamic contact angles were measured from each frame with GIMP 2 and ImageJ[30] analysis software package with the drop shape analysis plugin.[31] Reported values are averages of three measurements.

After observing effective self-actuated droplet motion on the dry surface, we verified droplets mobility on wet surface and estimated condensation efficiency. The surface is defined wet when it is cooled

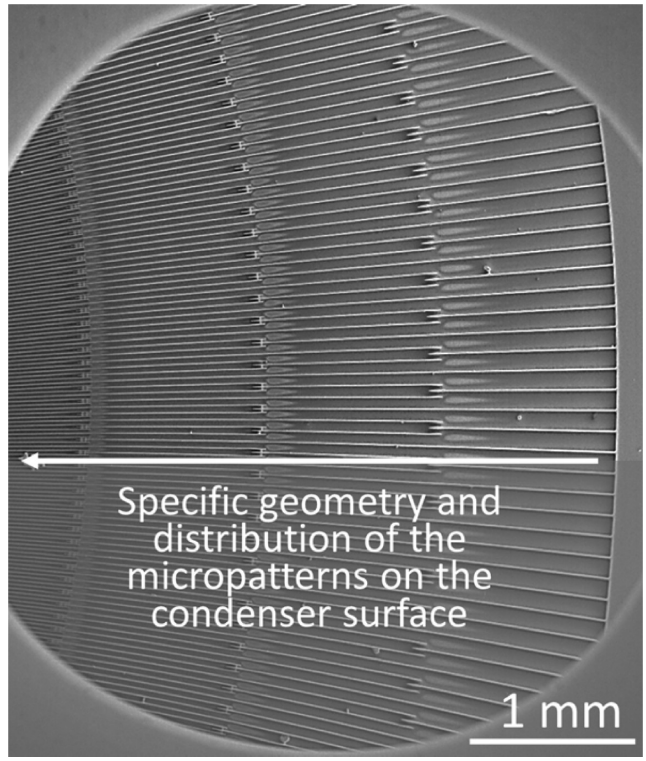

Figure 2. SEM image of the top view of the condenser surface. Only four outermost circular regions are shown due to the limited window of view of the microscope. Specific geometry and distribution of the micropatterns create a wettability gradient in the direction toward the center of the surface (as indicated with a white arrow).

below the ambient temperature and vapor condensation occurs on the surface. The condenser surface is cooled with a thermoelectric element (Custom Thermoelectric, part number: 12711-5L30-25CQ). The thermoelectric cooler is fixed with thermal grease to an aluminum block (143 × 102 × 23 mm), which serves as a heat sink to dissipate heat from the opposite side of the thermoelectric element. The condenser surface temperature is measured with a thermocouple attached to it and equals 14 °C. Relative humidity is estimated to 51% at measured dry (24 °C) and wet (17.4 °C) bulb temperatures. An LC Plus reusable nebulizer (part number: 022F81) is used to imitate the saturated air conditions. The water mass flow rate of the nebulizer is 440 mg/min. The mass median diameter of the droplets is 3.8 μm. The condenser surface is placed in proximity to the nebulizer outlet nozzle but is not contained in an enclosure with the nebulizer. The saturated air flow is positioned tangentially to the condenser surface to reduce effect of direct droplet deposition. We performed two sets of experiments to verify the self-cleaning property of the wet surface. The condensation efficiency of the self-cleaning surface is evaluated by mass and volume per area distribution as follows.

The total amount of collected condensate is found by subtracting the measured weight of the dry surface before the experiment from the weight of the wet surface at the end of the experiment. The effect of the self-cleaning property on condensation efficiency is analyzed by performing condensation tests in similar conditions with self-cleaning and plain hydrophobic surfaces. Both surfaces have the same hydrophobic coating and equal dimensions.

The volumetric condensate distribution was obtained from optical images of the condenser surface taken at the end of the condensation tests. Images were analyzed with ImageJ[30] software. Droplets areas are estimated based on their border profiles, as seen from above. The diameter of each droplet is estimated based on its profile area. The volume of each droplet is estimated as that of a hemisphere with the corresponding diameter. Reported values are averages from the three tests.

dx.doi.org/10.1021/la5004462 | *Langmuir* 2014, 30, 10133−10142

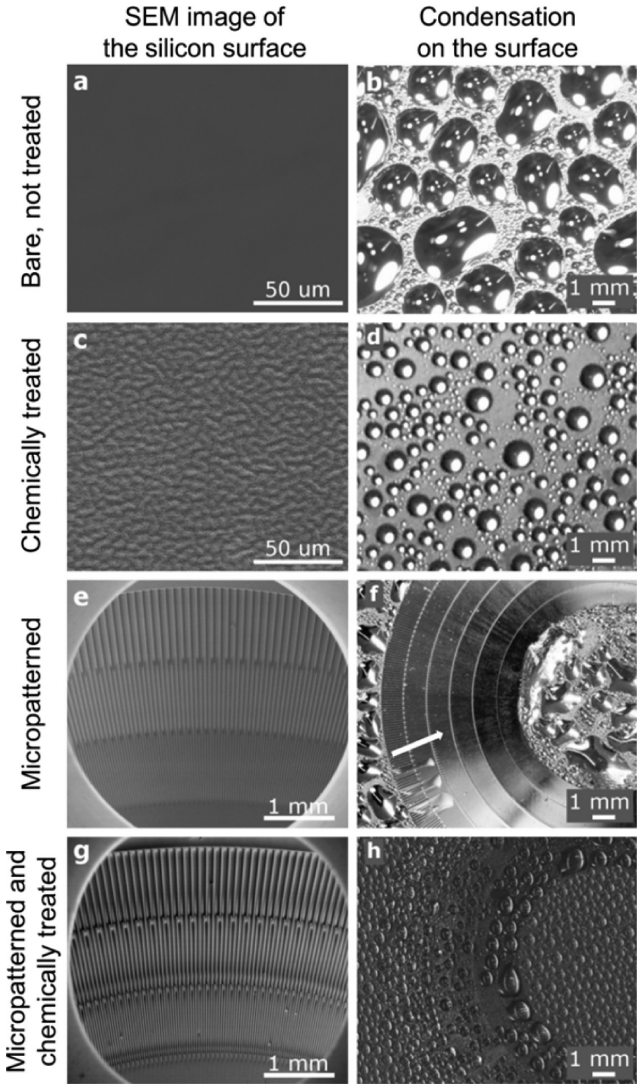

Figure 3. Comparison of condensation on four types of surfaces: step-by-step progress toward successful design of self-cleaning micro-condenser surface. (a) Unpatterned bare silicon surface. (b) The droplets are patch-like, wide at the base and low at height; they will form a liquid film once their border lines meet. (c) Chemically treated surface. (d) Droplets are spherical, extremely mobile but lack directional movement. (e) Micropatterned but not chemically treated surface. Surface hydrophobicity and wettability gradient are created with micropatterns. (f) The presence of wettability gradient is demonstrated with droplets spreading along the micropatterns (shown with white arrow). (g) The micropatterned surface is coated with plasma fluorinated polybutadiene film. (h) Dropwise condensation regime. Condensate droplets are self-collected at the inner edge of the micropatterned area.

■ RESULTS AND DISCUSSION

Condensation patterns on four types of surfaces are compared (Figure 3) under controlled conditions (temperature, humidity, and pressure), demonstrating a progression toward a self-cleaning condenser surface. The left-hand column images show the surfaces, and the right-hand column images show condensation on the corresponding surfaces. Patch-like condensation (Figure 3b) is observed on a bare silicon surface (Figure 3a); the droplets have large base diameters, 3−5 mm, and are flattened, 1 mm high. These droplets have low contact angle and are precursors of the formation of a liquid film that will cover the surface, once they coalesce. The condensation mode changes from filmwise to dropwise (Figure 3d) when the flat silicon surface is made hydrophobic by plasma fluorination of polybutadiene (Figure 3c).[27,29] From the side view, droplet profiles are spherical with diameters of 0.5−2.0 mm and have contact angles greater than 90°. Because of the high contact angle (122.2°) and low hysteresis, these droplets are unstable on the condenser surface (Figure 3d) and move erratically once the surface is disturbed from a horizontal position. This hydrophobic surface (Figure 3c) enhances dropwise condensation and droplet mobility but lacks directionality.

Micropatterning the surface with specifically designed and distributed microfeatures alters the surface energy[32] and creates a wettability gradient.[5] Figures 3e,f show the micropatterned silicon surface, which is not chemically treated, and condensation on it. The condensation regime is dropwise on the micropatterned region of the surface but patch-like on the unpatterned regions of the surface (center and beyond the outer edge of the patterned surface). The three stretched droplets sitting at the outer edge of the micropatterned area are in contact with the roughened region and spread along the wettability gradient along the two outer circular stages. Different condensation regimes and droplets propagation (extension) along the wettability gradient on hydrophobic surface suggest that roughening the surface with spatially oriented geometrical micropatterns distributed in a specific way increases surface hydrophobicity and creates a directional wettability gradient.

Condensation on the micropatterned and chemically treated surface (Figure 3g,h) demonstrates both dropwise condensation and directional droplet movement. We see dropwise condensation both on flat and micropatterned regions of the surface. The effect of the wettability gradient is demonstrated by the fact that the microdroplets self-collect at the inner edge of the micropatterned area. These droplets nucleate and grow throughout the surface and then move in the radial direction due to the imbalance of surface forces acting on the opposite sides of the contact line. These capillary forces are strong and can resist external forces. Video S2, in the Supporting Information, demonstrates that capillary forces can resist a flow of compressed air running at 4 m/s. The droplets are driven in the inward direction of the surface by capillary forces and resist an airflow directed in the, opposite, outward direction. Some droplets severely oscillate back and forth before they are blown off the surface.

Several criteria determine how readily droplets move on the surface upon condensation. High contact angle and low hysteresis are the key criteria but so is the distribution of the wettability gradient and the micropatterns geometry.[11] The micropatterns dimensions must be small enough to affect the movement of small condensate droplets. The critical diameter is defined as a minimum droplet base diameter, for a given length of a micropatterned region, below which capillary forces will not be able to actuate droplet movement. Usually, it is equal to twice the length of the surface topography features; i.e., a droplet will move only if its base contact line covers at least two regions with different wettability. The fluid and dimensions of the micropatterns determine the critical diameter of the droplet that will be affected by capillary forces. A researcher has to overcome the following difficulties when designing a self-cleaning condenser surface: creating an effective wettability gradient, optimizing the shape, dimensions, and packing of the microtopography features to provide a mechanism for

dx.doi.org/10.1021/la5004462 | Langmuir 2014, 30, 10133−10142

condensate droplets to transfer from Wenzel to Cassie wetting regime.

Increasing the condenser size is desired for providing sufficient surface area for condensation, but it increases the distance that a droplet has to travel toward the collection point which presents the challenge of defining an effective wettability distribution over a greater length. Simply increasing the radial length of each micropatterned region does not solve this problem because for a droplet to move its contact line must extend over at least two regions with different wettability.[33] Longer micropatterned regions will increase the critical diameter of the droplets. This will reduce the overall heat transfer because droplets in each region will stay immobile on the surface longer until they grow to the critical diameter. This will increase thermal resistance and reduce condensation efficiency.

Increasing the number of micropatterned regions reduces the radial length of each region and thus decreases the critical diameter of the droplets. But the difference in roughness between neighboring regions decreases, too, reducing the driving force to move a droplet from one region to the next. Hence, an optimal characteristic length must be determined such that it is small enough for the transport of droplets of various sizes and large enough to provide sufficient area for condensation.

The distributed size of condensate droplets, with volumes ranging from less than 1 μL to 4 μL, complicates the droplet transport problem as well. It is more difficult to transport smaller droplets over longer distances. A mechanism is needed to induce the movement of droplets smaller than the length of the region in which they are located. To address this, a trapezoidal geometry is selected for the ridges and grooves.

Condensation on micropatterned hydrophobic surfaces significantly increases contact angle hysteresis (CAH) which greatly affects droplet mobility,[8,9,34] creating an additional challenge in the design of a self-cleaning condenser surface. Droplets nucleate and grow in between and on top of micropatterns and must transit from a Wenzel[1] state (droplet fills the micropatterns) to a Cassie–Baxter[2] state (droplet sits on top of the micropatterns) upon condensation.[9] In the Cassie–Baxter state[5] the air–solid interface has a smaller energy barrier to droplet motion. Some surfaces completely lose their self-cleaning property upon condensation,[35] and others partly,[8] because droplets get pinned in between microstructures. The trapezoidal grooves and ridges of the surface, described here, allow droplets transition from a Wenzel to a Cassie–Baxter state[11,22] and enhance droplets coalescence. Zimmerman et al.[36] described the force balance due to the capillary pressures in the contracting microchannel. Capillary forces increase as the groove gets narrower in the inward radial direction which causes the droplets to move in the same direction[37] toward a location where the geometry is more favorable for the transition to a Cassie–Baxter state.[9,32] Droplets sitting on the top of the ridge move in the inward radial direction because of the increasing width (contact area increase) of the ridge toward the center of the surface. Thus, we design the combination of two physical phenomena: capillary pressure gradient and wettability gradient with trapezoidal geometry of the micropatterns. This geometry of the micropatterns is favorable even for droplets with base diameter much smaller than the critical diameter defined with the radial length of the micropatterns.

The novelty of this surface is that it provides a mechanism for droplet transition from "pinned" immobile to mobile state and promotes the transport of small condensed droplets over large distances. The insets in Figure 4a show micropatterns and droplet profiles for each circular region. Each region consists of a periodic arrangement of radially oriented ridges and grooves with the density of micropatterns increasing toward the center of the surface. The density of the micropatterns modulates surface wettability and is changed radially to establish the wettability gradient in the radial direction.[2,5,6,38] The wettability gradient is distributed between the most hydrophobic end of the surface (region six) and the least hydrophobic end (region one). Both ridges and grooves have trapezoidal profiles when observed from above; the ridges get wider and the grooves get narrower in the inward radial direction. This design creates a wettability gradient not only between the regions but also along the radial length of each micropatterned region, which enhances the movement of droplets with a base diameter smaller than the region length and improves the self-cleaning property of the surface.[11,22] To control the wettability, the dimensions of the ridges are kept constant for all six regions and the average width of the grooves is adjusted from region to region. The width of the grooves measured at the outer end of each region decreases from 110 μm in region six to 4 μm in region one. The grooves are approximately 60 μm deep. Each region is 1 mm wide in the radial direction; thus, the maximum distance that a droplet can travel from the outer edge of region six to the inner edge of region one is 6 mm. The measured contact angles decrease gradually from 157.0° to 126.7° toward the center of the condenser surface. The measured base diameter of the moving droplet increases from 0.6 to 1.1 mm as the droplet propagates from outward, most hydrophobic region, to the inward, least hydrophobic region. See Video S3 in the Supporting Information for more details on surface design and dimensions.

Figure 4b compares a designed, effective, contact angle distribution to a linear, ineffective, distribution. Reported static contact angle values are averages of four measurements taken at each circular micropatterned region; the error bars span three standard deviations. Actual measured data from our device are also shown. The micropatterns dimensions are modeled with the Cassie–Baxter model (eq 1) to yield an optimum "desired" contact angle distribution

$$\cos\theta_r^C = f_s(1 + \cos\theta_e) - 1 \quad (1)$$

where f_s is the ratio of the area that contacts the droplet to the projected area and θ_e is intrinsic contact angle, i.e., measured contact angle at the unpatterned surface with similar properties (122.2°). As the dimensions of micropatterns and surface hydrophobicity decrease, the ability of a droplet to be affected by a change in wettability decreases due to the increasing resistive forces.[7,38] Therefore, the effective wettability gradient distribution should not be linear[6] but increase in the inward radial direction for effective directional droplet movement. Droplets deposited at the outer edge of the micropatterned region stop at the third region where the wettability distribution is linear. Measured static contact angle values (Figure 4b) are lower than predicted by approximately 10°, but the shape of their distribution closely follows the designed one. The observed decrease in contact angle difference between the inner edge and region one as well as the linearity of the distribution in regions one and two are explained by our

dx.doi.org/10.1021/la5004462 | Langmuir 2014, 30, 10133–10142

technical limitation to fabricate microfeatures less than 2 μm at this high aspect ratio. We also note that while micropatterns in adjacent regions six through two are interleaved with each other, regions one and two are connected with no overlap.

Measured static contact angles show agreement with the values of the contact angles predicted with the Cassie−Baxter model. The contact angle values predicted with the Wenzel model (not shown here) deviate significantly from the measured data. This can be explained if the droplets on the surface of the sampler are lifted by the microasperities and have a liquid−vapor interface with the surface; i.e., the wetting mechanism is in the Cassie−Baxter mode.

The self-cleaning property of the wet surface was tested during condensation. Measurement of condensate mass, as described in the Methods section, shows that the self-cleaning property increases the amount of condensate by 5% in comparison to a plain hydrophobic surface. Greater condensate mass proves that there is a higher heat transfer rate between the moist air and the condenser surface. Figure 4c shows the volumetric distribution of condensate on the self-cleaning surface. Droplet movement toward the collection point during dropwise condensation was observed. Droplets collected at the inner edge of the micropatterned area (Figure 4c, inset). The total estimated volume, from the image analysis, shows agreement with the measured condensate mass. The volumetric distribution of condensate on the surface demonstrates the superior performance of the self-cleaning condenser versus plain hydrophobic surface. First, the self-cleaning surface routes condensate droplets in the predetermined direction. Second, the total condensate volume estimation, area under the curve, shows that self-cleaning surface collects 5% more condensate than a plane hydrophobic surface with similar dimensions. Droplet movement is postponed where the microfeatures' size is large because the droplets take longer to grow to the critical size. This explains the increase in volume per area in regions four through six. The data point at radius 3.5 mm corresponds to the volume per area distribution at the central flat region.

It is known that condensation efficiency depends on the wettability of the surface;[39,40] i.e., less hydrophobic surfaces have lower nucleation energy barrier than more hydrophobic surfaces. We should admit that the effect of hydrophobicity gradient in the shape of volume/area distribution, in Figure 4c, has not been completely elucidated in this experiment. We did not study what part of the variation in condensate volume distribution is due to the effect of hydrophobicity on the condensation rate itself. However, we note that the slight increase in condensation efficiency is in comparison to the plain hydrophobic surface with similar dimensions and chemical coating (Figure 3c,d). The plain (not micropatterned) surface (Figure 3c) is less hydrophobic (CA = 122.2°) than its micropatterned counterpart (Figure 3g) because roughening the surface increases its hydrophobicity, with CA ranging from 122.2° to 157.0°. Consequently the plain hydrophobic surface would be expected to exhibit a higher condensation rate if the rate depended only on the level of surface hydrophobicity. Our experiments show the opposite trend, which is consistent with a predominance of the self-cleaning property. Thus, it is very likely that the increase in condensation efficiency is solely due to the self-cleaning property of the surface rather than its hydrophobic gradient.

In order to obtain a better understanding of the droplet transition mechanism from the immobile nucleation to the moving state, we observed the condensation cycle under the optical microscope. The time-lapse images, shown in Figure 5, illustrate a continuous condensation cycle at microscale. This condensation experiment is conducted under similar temperature and humidity conditions as the previous experiment. See Video S4 in the Supporting Information to observe continuous condensation cycle captured under optical microscope. We can

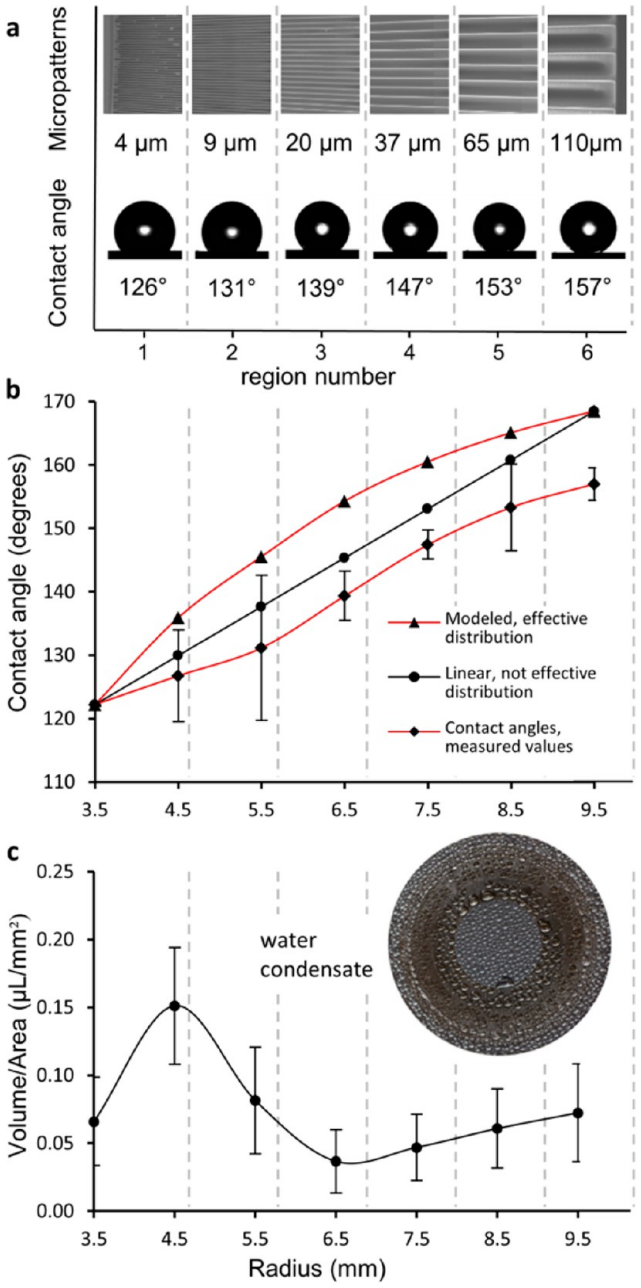

Figure 4. Surface topography, effective wettability gradient distribution, and self-cleaning property upon condensation. (a) SEM images of micropatterns at each region. The groove size decreases inward. Droplet profile and measured contact angle at each region. (b) Effective contact angles distribution, modeled with Cassie−Baxter model. Linear distribution is not effective, droplets stop at the third region. Measured distribution is effective, droplets flow from region six to region one. (c) Plot of volume/area distribution. Inset shows droplets distribution on the surface at the end of the condensation test. The volume per area at the central flat region corresponds to radius 3.5 mm. The lines connecting the data points in (b) and (c) are interpolating curves to guide the eye.

dx.doi.org/10.1021/la5004462 | *Langmuir* 2014, 30, 10133−10142

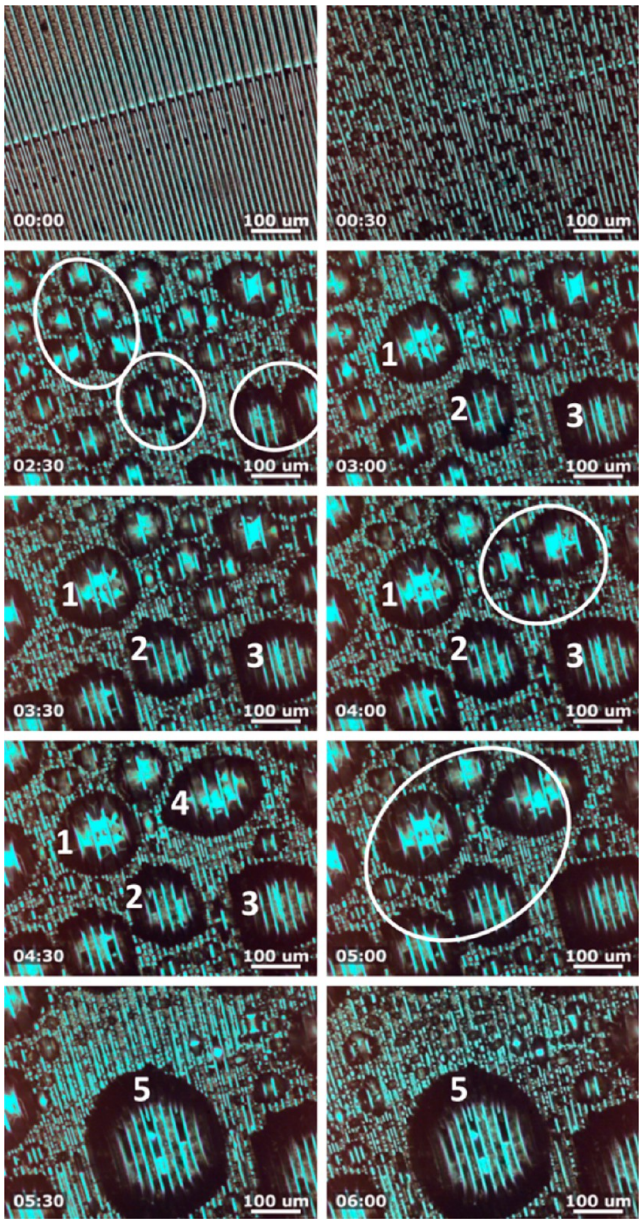

Figure 5. Continuous condensation cycle mechanism on self-cleaning condenser surface: droplet nucleation and growth (00:30, 02:30), local spreading (02:30, 03:00), and radial spreading (05:00, 05:30) to clear new sites for nucleation; new condensation cycle starts at previously occupied surface (06:00). Droplets clear the surface in the radial direction, which is toward bottom right corner. Ellipses show the droplets that unite into one (local spreading). Number labels indicate the droplets that underwent transition.

observe two key mechanisms: local spreading and radial spreading. Local spreading occurs when two or more stationary growing droplets merge with neighboring droplets. These droplets unite into one droplet which has a significantly larger diameter. The droplet starts moving along the wettability gradient toward the collection point if its diameter equals or exceeds the critical droplet diameter. Otherwise, it remains stationary, grows, or undergoes another series of local coalescences with its neighboring droplets until its contact line spreads over critical length and capillary forces actuate its movement. Radial spreading occurs when a droplet moving along the wettability gradient toward the collection point absorbs other droplets on its path. The volume of such droplet grows rapidly, which lets its contact line spread over regions with different wettability. Such droplet accelerates rapidly toward the collection point and clears multiple droplets from the condenser surface. Figure 5 demonstrates mechanism for continuous condensation cycle on hydrophobic self-cleaning surface. The first time frame shows dry condenser surface at the beginning of the experiment. Consecutive time frames demonstrate droplet nucleation and growth, local, and radial spreading. A group of droplets that undergo a series of local spreading events (frames 02:30 to 05:00) unite into one droplet and move in the radial direction (frame 05:30). New droplets start nucleation on previously occupied cite (frame 06:00), thus enhancing continuous condensation cycle. Droplet radial spreading is hard to capture under optical microscope since the area of view is limited. Droplet radial movement is evident at the macro scale. Such droplets swipe the surface in the radial direction; one can see a cleared path behind the droplet in the table of contents image.

We should give interpretation of the irregular shape of some droplets as observed from above under optical microscope, in Figure 5 and Video S4. We believe that they are not necessarily the consequence of contact angle hysteresis. We provided an evaluation of the contact angle hysteresis for droplets at the macro scale in Figure 4b. Each data point represents an average contact angle at each micropatterned circular region. These measurements show that it is negligible (3°−5°). The droplets that appear irregular at microscale are small (10−300 μm), early in their growth, right after nucleation. Initially, right after nucleation, these droplets are in the Wenzel state.[8,9] They transit to the Cassie state as they grow, which is confirmed by their near circular profiles afterward, and flow along the desired direction (Videos S2 and S4, at 5:24 and 6:07). Video S4 clearly demonstrates the effect of the capillary pressure gradient created with specific micropatterns geometry described earlier. In fact, we believe that this ability of the surface to promote transition from the Wenzel to Cassie state is the most important characteristic without which the self-cleaning property would not be possible.

The self-cleaning mechanism on condenser surface is more complicated than that on a dry surface on which a droplet is introduced and made to flow due to the presence of energy gradient on that surface. The contact angle hysteresis increases on the wetted micropatterned surface. The condensate droplets have very small and distributed diameters, ranging from 10 to 1000 μm. Two mechanisms are required: one to transfer nucleated droplets from a pinned to a mobile state, i.e., to aggregate a group of small neighboring droplets into one that is large enough to be affected by the wettability gradient and another to move those droplets along the wettability gradient. We described the mechanism for local coalescence, the aggregation of a group of droplets into one larger droplet, during the condensation cycle. Once these droplets undergo a series of local coalescences and the resulting droplet achieves the critical diameter, it will undergo radial coalescence. It starts moving toward the center of the surface, absorbing very small droplets on its path, along the wettability gradient. The critical droplet diameter is determined by the radial length of the micropatterns; in this design it is 1 mm. Thus, a droplet with a base diameter greater than 1 mm will flow due to the surface tension forces imbalance on its opposite sides. Figure 6 illustrates droplet mobility on a dry surface. Dynamic contact angle values, obtained from image frames extracted from the

dx.doi.org/10.1021/la5004462 | *Langmuir* 2014, 30, 10133−10142

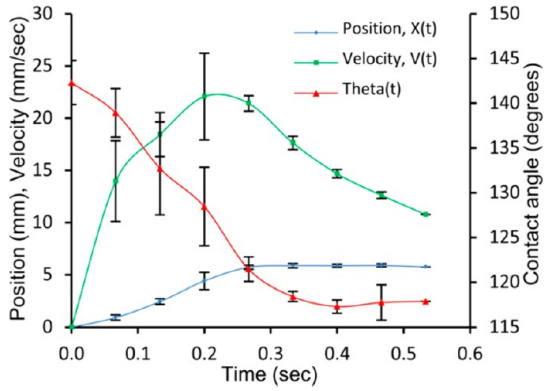

Figure 6. Droplet transport characterization on dry surface: contact angle, position, and velocity. The droplet is deposited on the outer region and is self-propulsed toward the center.

video files, as described in the Methods section, are commensurate with static contact angle measurements but different, as expected. This surface maintained reliable performance over multiple tests before its self-cleaning property degraded, mainly due to mechanical damage to the surface from handling.

To have an effective wettability gradient path that promotes the motion of deposited droplets is one of the initial requirements to a self-cleaning condenser surface. There are several approaches[6,7,38,41−43] to evaluate the capillary forces acting on the droplet in the presence of energy gradient. In this analysis, we assume that a droplet with a known volume is placed on dry micropatterned surface. The actuating and resistive forces acting on the moving droplet have to satisfy the second Newton's law of motion.

$$\sum F = (F_{\text{actuating}} - F_{\text{hysteresis}} - F_{\text{viscous}}) = ma \tag{2}$$

Daniel et al.[13] estimated the actuation force with the gradient of the surface free energy of adhesion of the droplet with the surface ($\Delta G = -\pi R^2 \gamma_{LV}(1 + \cos\theta_r)$)

$$F_{\text{actuating}} = -\frac{\mathrm{d}\Delta G}{\mathrm{d}x} \cong \pi {R_b}^2 \gamma_{LV}\left(\frac{\mathrm{d}}{\mathrm{d}x}\cos\theta_r\right) \tag{3}$$

A stable droplet has to overcome the static friction caused by interfacial contact before moving[33] and the reaction of viscous force during droplet motion. The resistance force comes from two sources: contact angle hysteresis, a droplet has to overcome the moving barrier before it begins to move, and viscous force during droplet motion. Furmidge[33] evaluated the hysteresis force as

$$F_{\text{hysteresis}} = 2 f_s R_b \gamma_{LV}(\cos\theta_R - \cos\theta_A) \tag{4}$$

where θ_R and θ_A are dynamic receding and advancing contact angles at the instant at which a droplet begins to move. The hysteresis force is related to the gradient of the total energy barrier defined in eqs 3−5.

Suda and Yamada[44] evaluated the resistive force resulting from the viscous effects.

$$F_{\text{viscous}} \cong 3\pi\eta R_b \bar{V} \ln\left(\frac{X_{\max}}{X_{\min}}\right) \tag{5}$$

where η is the fluid viscosity, $\bar{V}$ is the velocity of the moving droplet, and $X_{\max}$ and $X_{\min}$ are the characteristic lengths of a liquid. $X_{\max}$ is on the order of droplet radius (≈1 mm), and $X_{\min}$ is on the order of molecular dimension (≈0.1 nm). The net force acting on the droplet is defined as the sum of the three forces. We must note that surface condensation significantly complicates such analysis due to the changes in droplets volume, droplets coalescence, and greatly affected contact angle.

Figure 7 shows the distribution of the actuating, resistive, and net force over the surface with wettability gradient. This

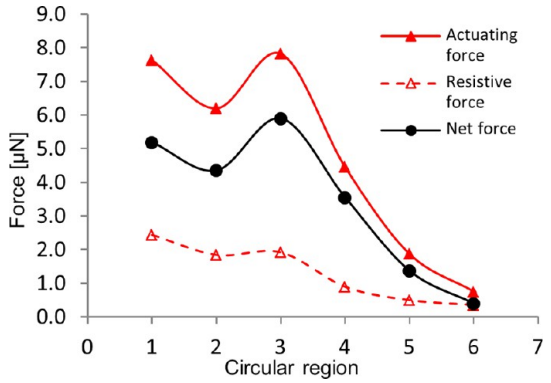

Figure 7. Distribution of actuating, resistive, and net force acting on the droplet over the six regions of the micropatterned surface. The magnitudes of forces are evaluated based on measured contact angles and dimensions of the micropatterns.

estimation is made based on the average of the four measurements of micropatterns dimensions (as fabricated) and measured contact angles. An average of the measured values is used because the dimensions of the fabricated topography features differ from the design values.

The forces distribution for experimental case has a similar trend as measured CA's distribution, shown in Figure 3b. The lack of interlocked connection of micropatterns between regions two and one significantly increases the resistive forces which affect the net driving force. In experiments, we observe that a deposited droplet accelerates rapidly and then slows down as it flows down the wettability gradient path. The droplet overcomes the resistive barrier at the interstage region because it acquired enough kinetic energy in the previous regions. This behavior is confirmed with Figure 6; it shows that a droplet accelerates initially and slows down at the end of the path.

We want to emphasize the importance of microtopography continuity when modeling the wettability gradient. The interface between two consecutive micropatterned regions has important effects on droplet transport. The regions must not be separated but have the geometry and dimensions that facilitate droplet motion from one region to the next. The packing density of micropatterns on these inter-region areas must not significantly vary from that of the two neighbor regions but be as close to their average as possible. Such distribution and agreement of microtopography features over the condenser surface will result in smoothly varying wettability gradient and effective droplet transport.

■ CONCLUSIONS

The goal of this work is the creation of a hydrophobic self-cleaning condenser surface with a directional self-cleaning property that can be used for collection of biological (chemical, environmental) samples or for condensation enhancement. The

dx.doi.org/10.1021/la5004462 | Langmuir 2014, 30, 10133−10142

goal is not, at this time, to demonstrate a significant increase in condensation efficiency. In this initial device, we achieve optimal performance with the simplest microfabrication process to ensure robustness and reliability. Our work offers insights into the design of a self-cleaning microcondenser surface, the effective wettability gradient distribution, and the micropatterns geometry. The self-cleaning property is demonstrated with droplet manipulation on the dry and wet, upon dropwise condensation, surfaces. Easy fabrication process and surface reliability may make this surface a good candidate for applications in biology and microfluidics. Future work may include maximizing the condensation rate and performance of microanalysis on the chip.

■ ASSOCIATED CONTENT

Supporting Information

Video S1 (cartoon) describes continuous droplet removal mechanism upon condensation and its benefits for high heat transfer and condensation efficiency. Video S2 (video) demonstrates that capillary forces can resist airflow of compressed air running at 4 m/s; the droplets are driven in the inward direction of the surface by capillary forces and resist an airflow directed in the outward direction; some droplets severely oscillate back and forth before they are blown off the surface. Video S3 (cartoon) describes surface design and dimensions as well as local and radial spreading mechanisms for droplet removal in continuous condensation cycle. Video S4 (video) demonstrates a continuous condensation cycle captured under optical microscope lens. The main steps in condensation cycle are observed: droplet nucleation, droplet growth, local spreading and radial spreading mechanisms to clear the surface. This material is available free of charge via the Internet at http://pubs.acs.org.

■ AUTHOR INFORMATION

Corresponding Author

*E-mail: cedavis@ucdavis.edu (C.E.D.).

Notes

The authors declare no competing financial interest.

■ ACKNOWLEDGMENTS

This work was generously supported by The Hartwell Foundation [C.E.D., J.P.D., N.J.K.]. Partial support was also provided by the United States Air Force Research Laboratory through contract FA8650-08-C-6832 and UES, Inc. [C.E.D., J.P.D., N.J.K., O.B.]. The project described was supported by the National Center for Advancing Translational Sciences (NCATS), National Institutes of Health (NIH), through grant #UL1 TR000002 [C.E.D., N.J.K.]. Graduate fellowship support [K.Z.] was provided by award number P42ES004699 from the National Institute of Environmental Health Sciences (NIEHS).

■ REFERENCES

(1) Wenzel, R. N. Surface roughness and contact angle. *J. Phys. Colloid Chem.* **1949**, *53* (9), 1466−1467.
(2) Cassie, A. B. D. Contact angles. *Trans. Faraday Soc.* **1948**, *44* (3), 11−16.
(3) Patankar, N. A. On the modeling of hydrophobic contact angles on rough surfaces. *Langmuir* **2003**, *19* (4), 1249−1253.
(4) He, B.; Patankar, N. A.; Lee, J. Multiple equilibrium droplet shapes and design criterion for rough hydrophobic surfaces. *Langmuir* **2003**, *19* (12), 4999−5003.
(5) Zhu, L.; Feng, Y. Y.; Ye, X. Y.; Zhou, Z. Y. Tuning wettability and getting superhydrophobic surface by controlling surface roughness with well-designed microstructures. *Sens. Actuators, A* **2006**, *130*, 595−600.
(6) Yang, J. T.; Chen, J. C.; Huang, K. J.; Yeh, J. A. Droplet manipulation on a hydrophobic textured surface with roughened patterns. *J. Microelectromech. Syst.* **2006**, *15* (3), 697−707.
(7) Yang, J. T.; Yang, Z. H.; Chen, C. Y.; Yao, D. J. Conversion of surface energy and manipulation of a single droplet across micropatterned surfaces. *Langmuir* **2008**, *24* (17), 9889−9897.
(8) Wier, K. A.; McCarthy, T. J. Condensation on ultrahydrophobic surfaces and its effect on droplet mobility: Ultrahydrophobic surfaces are not always water repellant. *Langmuir* **2006**, *22* (6), 2433−2436.
(9) Dorrer, C.; Ruhe, J. Condensation and wetting transitions on microstructured ultrahydrophobic surfaces. *Langmuir* **2007**, *23* (7), 3820−3824.
(10) Narhe, R. D.; Beysens, D. A., Nucleation and growth on a superhydrophobic grooved surface. *Phys. Rev. Lett.* **2004**, *93*, (7).
(11) Rykaczewski, K.; Paxson, A. T.; Anand, S.; Chen, X. M.; Wang, Z. K.; Varanasit, K. K. Multimode multidrop serial coalescence effects during condensation on hierarchical superhydrophobic surfaces. *Langmuir* **2013**, *29* (3), 881−891.
(12) Rykaczewski, K.; Scott, J. H. J.; Rajauria, S.; Chinn, J.; Chinn, A. M.; Jones, W. Three dimensional aspects of droplet coalescence during dropwise condensation on superhydrophobic surfaces. *Soft Matter* **2011**, *7* (19), 8749−8752.
(13) Daniel, S.; Chaudhury, M. K.; Chen, J. C. Past drop movements resulting from the phase change on a gradient surface. *Science* **2001**, *291* (5504), 633−636.
(14) Zhai, L.; Berg, M. C.; Cebeci, F. C.; Kim, Y.; Milwid, J. M.; Rubner, M. F.; Cohen, R. E. Patterned superhydrophobic surfaces: Toward a synthetic mimic of the Namib Desert beetle. *Nano Lett.* **2006**, *6* (6), 1213−1217.
(15) Chen, C. H.; Cai, Q. J.; Tsai, C. L.; Chen, C. L.; Xiong, G. Y.; Yu, Y.; Ren, Z. F. Dropwise condensation on superhydrophobic surfaces with two-tier roughness. *Appl. Phys. Lett.* **2007**, *90* (17), 173108.
(16) Dietz, C.; Rykaczewski, K.; Fedorov, A. G.; Joshi, Y. Visualization of droplet departure on a superhydrophobic surface and implications to heat transfer enhancement during dropwise condensation. *Appl. Phys. Lett.* **2010**, *97* (3), 033104.
(17) Boreyko, J. B.; Chen, C. H. Self-propelled dropwise condensate on superhydrophobic surfaces. *Phys. Rev. Lett.* **2009**, *103* (18), 184501.
(18) Narhe, R. D.; Beysens, D. A. Water condensation on a superhydrophobic spike surface. *Europhys. Lett.* **2006**, *75* (1), 98−104.
(19) Lau, K. K. S.; Bico, J.; Teo, K. B. K.; Chhowalla, M.; Amaratunga, G. A. J.; Milne, W. I.; McKinley, G. H.; Gleason, K. K. Superhydrophobic carbon nanotube forests. *Nano Lett.* **2003**, *3* (12), 1701−1705.
(20) Cheng, Y. T.; Rodak, D. E.; Angelopoulos, A.; Gacek, T. Microscopic observations of condensation of water on lotus leaves. *Appl. Phys. Lett.* **2005**, *87* (19), 194112.
(21) Yongfang Zhong, A. M. J.; Georgiadis, J. G. Condensation and wetting behavior on surfaces with microstructures: Super-hydrophobic and super-hydrophilic. *Int. Refrig. Air Cond. Conf.* **2006**, *R100*, P1.
(22) Feng, J.; Pang, Y. C.; Qin, Z. Q.; Ma, R. Y.; Yao, S. H. Why condensate drops can spontaneously move away on some superhydrophobic surfaces but not on others. *ACS Appl. Mater. Interfaces* **2012**, *4* (12), 6618−6625.
(23) Rose, J. W. Dropwise condensation theory and experiment: a review. *P I Mech. Eng. a-J. Pow* **2002**, *216* (A2), 115−128.
(24) Graham, C.; Griffith, P. Drop size distributions and heat-transfer in dropwise condensation. *Int. J. Heat Mass Transfer* **1973**, *16* (2), 337−346.
(25) Miljkovic, N.; Wang, E. N. Condensation heat transfer on superhydrophobic surfaces. *MRS Bull.* **2013**, *38* (5), 397−406.
(26) Miljkovic, N.; Enright, R.; Wang, E. N. Effect of droplet morphology on growth dynamics and heat transfer during

condensation on superhydrophobic nanostructured surfaces. *ACS Nano* **2012**, *6* (2), 1776−1785.
(27) Woodward, I.; Schofield, W. C. E.; Roucoules, V.; Badyal, J. P. S. Super-hydrophobic surfaces produced by plasma fluorination of polybutadiene films. *Langmuir* **2003**, *19* (8), 3432−3438.
(28) Bardaweel, H.; Zamuruyev, K.; Delplanque, J. P.; Kenyon, N. J.; Carron, C.; Brand, O.; Davis, C. E. In *Microscale Surface Energy Properties for Enhanced Surface Condensation and Sampling of Exhaled Breath Metabolites, Hilton Head Island, SC, 3−7 June 2012*; Mehregany, M. D., Ed.; 2012; pp 239−242.
(29) Woodward, I. S.; Schofield, W. C. E.; Roucoules, V.; Bradley, T. J.; Badyal, J. P. S. Micropatterning of plasma fluorinated super-hydrophobic surfaces. *Plasma Chem. Plasma Process.* **2006**, *26* (5), 507−516.
(30) Rasband, W. S. ImageJ; http://rsb.info.nih.gov/ij/.
(31) Stalder, A. Drop shape analysis plugin; http://bigwww.epfl.ch/demo/dropanalysis/.
(32) Enright, R.; Miljkovic, N.; Al-Obeidi, A.; Thompson, C. V.; Wang, E. N. Condensation on superhydrophobic surfaces: The role of local energy barriers and structure length scale. *Langmuir* **2012**, *28* (40), 14424−14432.
(33) Furmidge, C. G. Studies at phase interfaces. 1. Sliding of liquid drops on solid surfaces and a theory for spray retention. *J. Coll. Sci., Imp. Univ. Tokyo* **1962**, *17* (4), 309.
(34) Cheng, Y. T.; Rodak, D. E. Is the lotus leaf superhydrophobic? *Appl. Phys. Lett.* **2005**, *86* (14), 144101.
(35) Guo, Z. G.; Liu, W. M.; Su, B. L. Superhydrophobic surfaces: From natural to biomimetic to functional. *J. Colloid Interface Sci.* **2011**, *353* (2), 335−355.
(36) Zimmermann, M.; Schmid, H.; Hunziker, P.; Delamarche, E. Capillary pumps for autonomous capillary systems. *Lab Chip* **2007**, *7* (1), 119−125.
(37) Al-Housseiny, T. T.; Tsai, P. C. A.; Stone, H. A. Control of interfacial instabilities using flow geometry. *Nat. Phys.* **2012**, *8* (10), 747−750.
(38) Fang, G. P.; Li, W.; Wang, X. F.; Qiao, G. J. Droplet motion on designed microtextured superhydrophobic surfaces with tunable wettability. *Langmuir* **2008**, *24* (20), 11651−11660.
(39) Zhao, H.; Beysens, D. From droplet growth to film growth on a heterogeneous surface - Condensation associated with a wettability gradient. *Langmuir* **1995**, *11* (2), 627−634.
(40) Varanasi, K. K.; Hsu, M.; Bhate, N.; Yang, W. S.; Deng, T. Spatial control in the heterogeneous nucleation of water. *Appl. Phys. Lett.* **2009**, *95* (9), 094101.
(41) Li, W.; Amirfazli, A. Microtextured superhydrophobic surfaces: A thermodynarnic analysis. *Adv. Colloid Interface Sci.* **2007**, *132* (2), 51−68.
(42) Subramanian, R. S.; Moumen, N.; McLaughlin, J. B. Motion of a drop on a solid surface due to a wettability gradient. *Langmuir* **2005**, *21* (25), 11844−11849.
(43) Li, W.; Amirfazli, A. Microtextured superhydrophobic surfaces: a thermodynamic analysis. *Adv. Colloid Interface Sci.* **2007**, *132* (2), 51−68.
(44) Suda, H.; Yamada, S. Force measurements for the movement of a water drop on a surface with a surface tension gradient. *Langmuir* **2003**, *19* (3), 529−531.